

Electronically Dissymmetric DIPHOS Derivatives Give Higher n:i Regioselectivity in Rhodium-Catalyzed Hydroformylation Than Either of Their Symmetric Counterparts

Charles P. Casey,* Evelyn Lin Paulsen, Eckart W. Beuttenmueller, Bernd R. Proft, Brock A. Matter, and Douglas R. Powell

Contribution from the Department of Chemistry, University of Wisconsin, Madison, Wisconsin 53706

Received June 18, 1998

Abstract: Electronic effects on rhodium-catalyzed hydroformylation of 1-hexene with electronically dissymmetric DIPHOS derivatives [3,5-(CF₃)₂C₆H₃]₂PCH₂CH₂PPh₂ = [DIPHOS-(3,5-CF₃,H)] (1), [2-(CF₃)C₆H₄]₂PCH₂CH₂PPh₂ = [DIPHOS-(2-CF₃,H)] (2), [3,5-(CF₃)₂C₆H₃]₂PCH₂CH₂P[2-(CH₃)C₆H₄]₂ = [DIPHOS-(3,5-CF₃,2-CH₃)] (3), and [2-(CF₃)C₆H₄]₂PCH₂CH₂P[2-(CH₃)C₆H₄]₂ = [DIPHOS-(2-CF₃,2-CH₃)] (4) were investigated. Two apical–equatorial chelate isomers were observed for model (diphosphine)Ir(CO)₂H complexes of dissymmetric diphosphines 1–4. In each case, the equatorial phosphine of the major isomer (96–60%) had electron-withdrawing aryl substituents. These dissymmetric DIPHOS derivatives were used to test the hypothesis that an electron-withdrawing substituent on an equatorial phosphine increases the hydroformylation n:i ratio while an electron-withdrawing substituent on an apical phosphine decreases the n:i ratio. In agreement with the predictions of this hypothesis, hydroformylation with the dissymmetric diphosphine ligand DIPHOS-(3,5-CF₃,H) (1), gave an n:i ratio of 4.2:1, higher than either of the symmetric ligands DIPHOS, 2.6:1, and DIPHOS-(3,5-CF₃), 1.3:1. Similar observations were made for hydroformylations with 2–4.

The rhodium–phosphine-catalyzed hydroformylation reaction,¹ first reported by Wilkinson² in the late 1960s and implemented by Union Carbide³ in the late 1970s, remains one of the most important homogeneously catalyzed processes. Rhodium–phosphine catalysts operate at lower temperature and pressure than earlier cobalt-based catalysts and afford the opportunity to maximize regioselectivity with ancillary phosphine ligand variations. The development of highly regioselective catalyst systems continues to be a primary research aim. Recently developed phosphorus chelates which give high regioselectivity for high linear aldehydes include Texas-Eastman's 2,2'-bis[(diphenylphosphino)methyl]-1,1'-biphenyl (BISBI) ligand⁴ and Union Carbide's diphosphite chelates.⁵ Stanley has developed a unique binuclear rhodium catalyst that gives high rates and selectivity.⁶ van Leeuwen has reported a

variety of diphosphite and diphosphine ligands that give high n:i regioselectivity.⁷ Buchwald⁸ and Wink⁹ have obtained high regioselectivities in hydroformylation of functionalized alkenes using rhodium diphosphite systems. While a wide variety of phosphine and phosphite ligands have been screened, no detailed understanding of how phosphorus ligands control regioselectivity or enantioselectivity has emerged.

Wilkinson's dissociative hydroformylation mechanism (Scheme 1) suggests that aldehyde regioselectivity is determined in the hydride addition step that converts a five-coordinate H(alkene)-Rh(CO)L₂ into either a primary or secondary four-coordinate (alkyl)Rh(CO)L₂. Monodentate phosphine ligands can occupy two equatorial or one equatorial and one apical site of the key five-coordinate H(alkene)Rh(CO)L₂ intermediate. For L = PPh₃, Brown's NMR studies showed an 85:15 diequatorial:apical–equatorial mixture of isomers of (PPh₃)₂Rh(CO)₂H which are in rapid equilibrium at room temperature.¹⁰

Several years ago, on the basis of Brown's findings, we set out to test the hypothesis that very different regioselectivities

(1) (a) Parshall, G. W. *Homogeneous Catalysis: The Applications and Chemistry of Catalysis by Soluble Transition Metal Complexes*; Wiley: New York, 1980. (b) Tkatchenko, I. In *Comprehensive Organometallic Chemistry*; Wilkinson, G., Stone, F. G. A., Abel, E. W., Eds.; Pergamon: Oxford, 1982; Vol. 8, pp 101–223. (c) Tolman, C. A.; Faller, J. W. In *Homogeneous Catalysis with Metal Phosphine Complexes*; Pignolet, L. H., Ed.; Plenum: New York, 1983; pp 81–109. (d) Pino, P.; Piacenti, F.; Bianchi, M. In *Organic Syntheses via Metal Carbonyls*; Wender, I., Pino, P., Eds.; Wiley-Interscience: New York, 1977; Vol. 2, pp 136–197. (e) Consiglio, G.; Pino, P. *Top. Curr. Chem.* **1982**, *105*, 77. (f) Beller, M.; Cornils, B.; Frohning, C. D.; Kohlpaintner, C. W. *J. Mol. Catal. A* **1995**, *104*, 17–85.

(2) (a) Evans, D.; Osborn, J. A.; Wilkinson, G. *J. Chem. Soc. A* **1968**, 3133. (b) Yagupsky, G.; Brown, C. K.; Wilkinson, G. *J. Chem. Soc. A* **1970**, 1392. (c) Brown, C. K.; Wilkinson, G. *J. Chem. Soc. A* **1970**, 2753.

(3) Pruet, R. L. *Ann. N.Y. Acad. Sci.* **1977**, *295*, 239.
(4) (a) Devon, T. J.; Phillips, G. W.; Puckette, T. A.; Stavinoha, J. L.; Vanderbilt, J. J. (to Texas-Eastman). U.S. Patent 4,694,109, 1987; *Chem Abstr.* **1988**, *108*, 7890. For closely related systems, see: (b) Devon, T. J.; Phillips, G. W.; Puckette, T. A.; Stavinoha, J. L.; Vanderbilt, J. J. (to Texas-Eastman) U.S. Patent 5,332,846, 1994; *Chem Abstr.* **1994**, *121*, 280,879. (c) Bahrmann, H.; Lappe, P.; Herrmann, W. A.; Albanese, G. P.; Manetsberger, R. B. (to Hoechst AG) DE Patent 4,333,307, 1995; *Chem Abstr.* **1995**, *123*, 112,408.

(5) (a) Billig, E.; Abatjoglou, A. G.; Bryant, D. R. (to Union Carbide) U.S. Patent 4,748,261 1988; 4,769,498, 1988. (b) For related work with phosphine–phosphite chelates, see: Nozaki, K.; Sakai, N.; Nanno, T.; Higashijima, T.; Mano, S.; Horiuchi, T.; Takaya, H. *J. Am. Chem. Soc.* **1997**, *119*, 4413.

(6) Broussard, M. E.; Juma, B.; Train, S. G.; Peng, W.-J.; Laneman, S. A.; Stanley, G. G. *Science* **1993**, *260*, 1784.

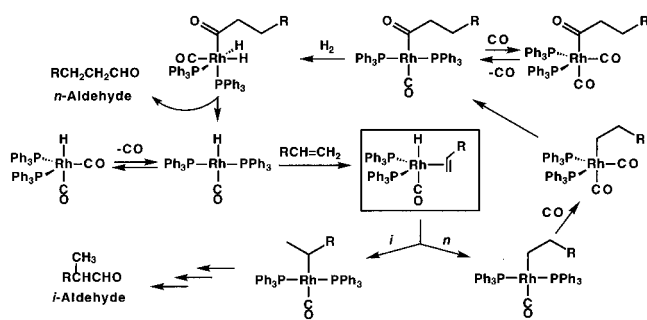
(7) (a) van Rooy, A.; Kamer, P. C. J.; van Leeuwen, P. W. N. M.; Goubitz, K.; Fraanje, J.; Veldman, N.; Spek, A. L. *Organometallics* **1996**, *15*, 835. (b) Buisman, G. J. H.; Martin, M. E.; Vos, E. J.; Klootwijk, A.; Kamer, P. C. J.; van Leeuwen, P. W. N. M. *Tetrahedron: Asymmetry* **1995**, *6*, 719. (c) Kranenburg, M.; van der Burgt, Y. E. M.; Kamer, P. C. J.; van Leeuwen, P. W. N. M.; Goubitz, K.; Fraanje, J. *Organometallics* **1995**, *14*, 3081.

(8) Cuny, G. D.; Buchwald S. L. *J. Am. Chem. Soc.* **1993**, *115*, 2066.

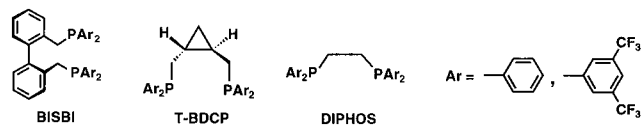
(9) Kwok, T. J.; Wink, D. J. *Organometallics* **1993**, *12*, 1954.

(10) Brown, J. W.; Kent, A. G. *J. Chem. Soc., Perkin Trans. 2* **1987**, 1597.

Scheme 1



might be obtained from diequatorial diphosphine rhodium complexes and from apical–equatorial diphosphine rhodium complexes. The mode of chelation could be controlled by employing chelating diphosphines with varying natural bite angles.¹¹ A strong correlation was found between regioselectivity for *n*-aldehyde formation and natural bite angle.¹² Chelates such as BISBI with wide natural bite angles gave a much higher percent *n*-aldehyde ($\beta_n = 113^\circ$, *n*:*i* = 66) than diphosphines such as 1,2-bis(diphenylphosphino)ethane (DIPHOS) with narrow bite angles ($\beta_n = 85^\circ$, *n*:*i* = 2.6).^{13,14} Deuterioformylation studies established that the predominant products were derived from irreversible addition of a rhodium hydride to a complexed alkene to give a rhodium alkyl intermediate that is committed to aldehyde formation.¹⁵



The correlation between regioselectivity and chelation mode suggests that diequatorial diphosphines such as BISBI and apical–equatorial chelating diphosphines such as DIPHOS have significantly different steric and/or electronic properties. We first considered the steric differences between diequatorial and apical–equatorial chelates as a possible explanation for regioselectivity. Molecular mechanics calculations were employed to explore whether selectivity arose from steric differences between the transition states leading to the primary and secondary alkyrhodium intermediates.¹⁵ Unfortunately these models predicted higher *n*:*i* regioselectivity for DIPHOS (predicted 35:1, observed 2.6:1) than for BISBI (predicted 25:1, observed 66:1), contrary to our observations. These estimates of steric effects incorrectly suggested that DIPHOS should be more selective than BISBI, which is in fact the opposite of the trend observed.

Since steric arguments failed to give a satisfactory explanation for the much higher *n*:*i* aldehyde ratios observed, next we focused on investigating electronic effects.¹⁶ We tested a series

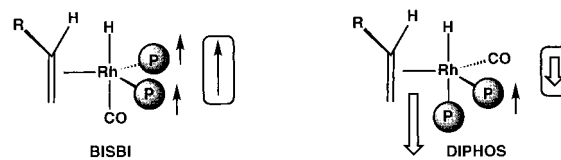


Figure 1. Effect of equatorial and apical electron-withdrawing groups on *n*:*i* selectivity. For BISBI, the effect of electron-withdrawing groups on each of the two equatorial phosphines increases the *n*:*i* selectivity to give a net additive increase in *n*:*i* selectivity shown in the box. For DIPHOS, the effect of electron-withdrawing groups on the equatorial phosphine increases the *n*:*i* selectivity, but the effect of electron-withdrawing substituents on the apical phosphine decreases the *n*:*i* selectivity to a greater degree; the resulting net decrease in *n*:*i* selectivity is shown in the box.

of symmetrically substituted diphosphines with different chelation modes and varied the electronic environment at the arylphosphino group.

We found that the added electron-withdrawing aryl substituents of BISBI–(3,5- CF_3) and T-BDCP–(3,5- CF_3) ligand, coordinated diequatorially on model five-coordinate metal complexes, led to an increase in the linear to branched (*n*:*i*) ratio. From the BISBI–(3,5- CF_3) and T-BDCP–(3,5- CF_3) data, we were able to deduce that electron-withdrawing aryl substituents in the equatorial position increased the *n*:*i* selectivity. However, the DIPHOS–(3,5- CF_3) ligand, which coordinates in an apical–equatorial mode, showed a decrease in the *n*:*i* ratio with electron-withdrawing aryl substituents. If electron-withdrawing aryl substituents in the equatorial position increase *n*:*i* selectivity, then in order to obtain a decrease in *n*:*i* selectivity for the apical–equatorial chelated DIPHOS–(3,5- CF_3), the electron-withdrawing aryl substituents in the apical position must act to decrease *n*:*i* selectivity. Our hypothesis then is that an electron-withdrawing substituent on an equatorial phosphine increases the *n*:*i* ratio while an electron-withdrawing substituent on an apical phosphine decreases the *n*:*i* ratio (Figure 1).

A risky prediction of our hypothesis is that using the dissymmetric DIPHOS derivative [3,5-(CF_3) $_2\text{C}_6\text{H}_3$] $_2\text{PCH}_2\text{CH}_2\text{PPh}_2 = [\text{DIPHOS}-(3,5-\text{CF}_3, \text{H})]$ could lead to greater *n*:*i* selectivity than either of the related symmetric DIPHOS derivatives [DIPHOS–(3,5- CF_3) or DIPHOS]. This chelate is designed to have an electron-withdrawing phosphine in the equatorial position and an electron-donating phosphine in the apical position. Here we report the synthesis and characterization of [DIPHOS–(3,5- $\text{CF}_3, \text{H})]$ and several other dissymmetric DIPHOS derivatives as well as their chelation mode in model (diphosphine)Ir(CO) $_2$ H complexes. It was determined that hydroformylation *n*:*i* selectivity with these derivatives is indeed greater than either of their related symmetric DIPHOS derivatives, supporting our hypothesis.

Results

Synthesis of Electronically Dissymmetric DIPHOS Derivatives. Electronically dissymmetric DIPHOS derivatives containing both an electron-donating aryl substituent (H or *o*- CH_3) and an electron-withdrawing aryl substituent [*o*- CF_3 or bis-*m*-(CF_3) $_2$] were synthesized by the base-catalyzed addition¹⁷ of a secondary arylphosphine¹⁶ to a diarylvinylphosphine¹⁶ in moderate yields (16–61%) (Scheme 2, Figure 2). The reaction of electron-rich arylphosphines with electron-poor vinylphosphines gave the desired ligands. In some cases, the reverse

(11) Casey, C. P.; Whiteker, G. T. *Isr. J. Chem.* **1990**, *30*, 299.

(12) Casey, C. P.; Whiteker, G. T.; Melville, M. G.; Petrovich, L. M.; Gavney, J. A., Jr.; Powell, D. R. *J. Am. Chem. Soc.* **1992**, *114*, 5535.

(13) van Leeuwen also observed an increase in linear aldehyde regioselectivity with increasing bite angle.^{7c} In a series of bidentate chelating phosphines containing xanthene-like ligand backbones, the bite angle was varied from 102° to 131° , with minimal change in the steric or electronic properties of the ligand. The resulting *n*:*i* ratio increased from 6.7 to 80.5 in the hydroformylation of 1-octene at 80°C .

(14) Earlier we reported a 2.1:1 *n*:*i* ratio for DIPHOS,¹² which is the ratio seen early in the reaction. For consistency, we are now reporting ratios obtained after 120–250 turnovers (20–50% conversion) for all ligands.

(15) Casey, C. P.; Petrovich, L. M. *J. Am. Chem. Soc.* **1995**, *117*, 6007.

(16) Casey, C. P.; Paulsen, E. L.; Beuttenmueller, E. W.; Proft, B. R.; Petrovich, L. M.; Matter, B. A.; Powell, D. R. *J. Am. Chem. Soc.* **1997**, *119*, 11817.

(17) (a) Clark, P. W.; Mulroney, B. J. *J. Organomet. Chem.* **1981**, *217*, 51. (b) Chatt, J.; Hussain, W.; Leigh, G. J.; Ali, H. M.; Pickett, C. J.; Rankin, D. A. *J. Chem. Soc., Dalton Trans.* **1985**, 1131.

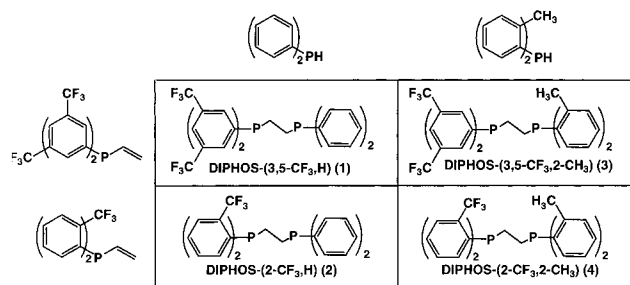
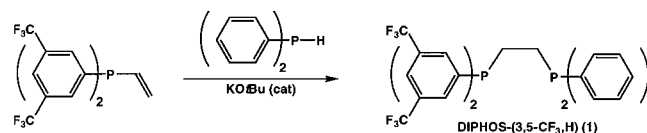


Figure 2. Starting materials for dissymmetric DIPHOS derivatives 1–4.

Scheme 2

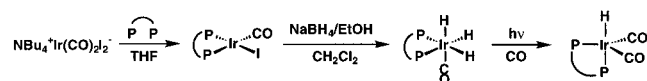


combination failed. For example, (2-CF₃C₆H₄)₂PH and (C₆H₅)₂P(CH=CH₂) did not give DIPHOS-(2-CF₃,H) (2).

Synthesis of Iridium Complexes as Models of Catalytic Species. The nature of the catalytic rhodium hydride alkene intermediate is important in understanding aldehyde regioselectivity. Insertion of the rhodium hydride into the terminal or internal alkene carbon–hydrogen bond is the regioselectivity-determining step for aldehyde formation. However, this catalytic rhodium hydride alkene intermediate has never been directly observed due to rapid hydride insertion to give a rhodium alkyl species. The similar chelating diphosphine rhodium dicarbonyl hydride where the alkene is replaced by a carbonyl is a suitable model; however, it was not employed because in many cases such complexes are unstable relative to loss of hydrogen and dimer formation.¹⁸ Therefore, diphosphine iridium dicarbonyl hydride complexes were used to determine the diphosphine chelate geometry in a five-coordinate metal complex. Iridium is a good model for rhodium complexes because it has similar coordination geometries and iridium bond lengths are only 1–2% longer than related rhodium bond lengths.

(Diphosphine)Ir(CO)₂H complexes were prepared from diphosphines 2–4 (Scheme 3). The NaBH₄ addition to (diphosphine)Ir(CO)I complexes gave the trihydrides, *fac*-(diphosphine)Ir(CO)H₃. Subsequent photolysis under CO gave the desired (diphosphine)Ir(CO)₂H complexes.¹⁹

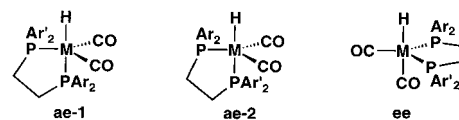
Scheme 3



An alternative method was necessary for (DIPHOS-3,5-CF₃,H)Ir(CO)₂H (5). The (DIPHOS-3,5-CF₃,H)Ir(CO)I complex which is normally precipitated out with the addition of ethanol remained soluble, and therefore could not be separated from unreacted starting materials. Therefore, the dicarbonyl complex was synthesized directly by reaction with Ir(acac)(CO)₂ under 1 atm of 1:1 CO:H₂.

Coordination Geometry of (Diphosphine)Ir(CO)₂H Complexes. These model compounds are particularly important in understanding the mode of chelation for dissymmetric complexes. For a dissymmetric diphosphine, there are three isomers

of (diphosphine)Ir(CO)₂H: one diequatorial isomer (**ee**) and two apical–equatorial isomers (**ae-1**, **ae-2**). The parent diphosphine DIPHOS has a calculated natural bite angle of 84.5°, thus making apical–equatorial (**ae**) chelation strongly preferred.



The two apical–equatorial isomers, **ae-1** and **ae-2**, undergo rapid interconversion by a series of Berry pseudorotations, giving averaged NMR signals at room temperature.²⁰ The NMR spectra for the individual isomers can be observed at low temperature, where interconversion is slow on the NMR time scale.³¹ ³¹P chemical shifts of the isomers can be assigned by comparison of shifts in dissymmetric complexes with the corresponding shifts for the symmetric complexes, while selectively hydride coupled ³¹P spectra can be used to determine the site of phosphine binding (Table 1). Apical bound phosphines show a large P–H coupling constant to the apical hydride in the range of 90–110 Hz. The equatorial P–H coupling is usually around –15 Hz which can result in ³¹P resonance broadening for equatorial bound phosphines (Table 1).

[DIPHOS-(3,5-CF₃,H)]Ir(CO)₂H (5). The ¹H and ³¹P NMR spectra of **5** at –94 °C revealed the presence of two isomers in a 94:6 ratio (Figure 3). The major isomer had ³¹P NMR resonances at δ 38.7 and 31.6 ppm and a hydride resonance in the ¹H NMR spectrum at δ –11.21 (dd, *J*_{HP} = 91.5, –14.5 Hz). The minor isomer had ³¹P resonances at δ 36.7 and 34.0 ppm and a hydride resonance at δ –11.12 (dd, *J*_{HP} = 100, –15 Hz). The observation of one large trans *J*_{HP} coupling and one small cis *J*_{HP} coupling established that each isomer had apical–equatorial diphosphine coordination. In the hydride-coupled ³¹P NMR spectrum of the major isomer, the resonance at δ 31.6 had a large coupling to a trans hydride (*J*_{HP} = 87 Hz). In the hydride-coupled ³¹P NMR spectrum of the minor isomer, the resonance at δ 36.7 also had a large coupling to a trans hydride (*J*_{HP} = 87 Hz).

The structural assignments of isomers **5a** and **5b** were made by comparison of chemical shifts with analogous symmetric DIPHOS iridium complexes (Figure 3, Table 1). For the major isomer, the δ 31.6 chemical shift of the apical phosphorus trans to hydride (*J*_{HP} = 87 Hz) is the same as the δ 31.6 (*J*_{HP} = 85 Hz) chemical shift of the apical phosphorus of (DIPHOS)Ir(CO)₂H and the δ 38.7 chemical shift of its equatorial phosphorus cis to hydride (*J*_{HP} = 9.5 Hz) is similar to the δ 39.2 (br s) of the equatorial phosphine of (DIPHOS-3,5-CF₃)Ir(CO)₂H. This establishes the structure of the major isomer as **5a** with the electron-withdrawing PAR₂ group in an equatorial position. Similarly, for the minor isomer, the δ 36.7 chemical

(20) We agree with van Leeuwen's suggestion^{20a,b} that equilibration of isomers such as **ae-1** and **ae-2** does not occur via a Berry pseudorotation involving pivoting about the equatorial phosphine; such a pseudorotation would proceed through an unstable intermediate with both an unfavorable equatorial hydride and a small bite angle chelate spanning equatorial sites. However, a series of Berry pseudorotations involving successive pivoting about CO, H, and CO avoids diequatorial diphosphines and appears likely, even though it requires an intermediate with an equatorial hydride ligand. We cannot exclude a one-step Meakin mechanism^{20c} for phosphine interchange. The transition state for Berry pseudorotation is a square-based pyramid that we believe would be more stable than the transition state for a Meakin mechanism which resembles an edge-protonated tetrahedron. (a) Buisman, G. J. H.; van der Veen, L. A.; Kamer, P. C. J.; van Leeuwen, P. W. N. M. *Organometallics* **1997**, *16*, 5681–5687. (b) Castellanos-Páez, A.; Castillón, S.; Claver, C.; van Leeuwen, P. W. N. M.; de Lange, W. G. J. *Organometallics* **1998**, *17*, 2543–2552. (c) Meakin, P.; Muettterties, E. L.; Jesson, J. P. *J. Am. Chem. Soc.* **1972**, *94*, 5271.

(18) For example, attempts to synthesize (T-BDCP)Rh(CO)₂H led to [(T-BDCP)Rh]₂(μ-CO)₂.¹²

(19) (a) Fisher, B. J.; Eisenberg, R. *Organometallics* **1983**, *2*, 764. (b) Fisher, B. J.; Eisenberg, R. *Inorg. Chem.* **1984**, *23*, 3216.

Table 1. Low-Temperature ^{31}P (Selectively Hydride Coupled) and ^1H Hydride NMR Chemical Shifts for (Diphosphine) $\text{Ir}(\text{CO})_2\text{H}$ Complexes

| diphosphine | major equatorial P | major apical P | minor equatorial P | minor apical P | major hydride | minor hydride |
|---|-------------------------|------------------------------|--------------------|---------------------------|------------------------------------|---------------------------------|
| Symmetric ^a | | | | | | |
| DIPHOS | 33.6 (t, $J = 12$) | 31.6 (dd, $J = 85, -10$) | | | -11.20 (dd, $J = 92, -13$) | |
| DIPHOS-(3,5-CF ₃) | 39.2 (br s) | 37.4 (br d, $J = 103$) | | | -10.97 (dd, $J = 101, -14$) | |
| DIPHOS-(2-CH ₃) | 26.9 (br s) | 25.4 (br d, $J = 83$) | | | -11.38 (dd, $J = 98, -16$) | |
| DIPHOS-(2-CF ₃) | 37.6 (br s) | 33.0 (br d, $J = 104$) | | | -11.41 (dd, $J = 105, -14$) | |
| Unsymmetric | | | | | | |
| DIPHOS-(3,5-CF ₃ ,H) (5) | 38.7 (t, $J = 9.5$) | 31.6 (dd, $J = 87, 9$) | 34.0 (br s) | 36.7 (br d, $J = 87$) | -11.21 (dd, $J = 91.5, -14.5$) | -11.12 (dd, $J = 100, -14$) |
| DIPHOS-(2-CF ₃ ,H) (6) | 40.5 (s) | 34.0 (d, $J = 92$) | H | 3,5-CF ₃ | -10.69 (dd, $J = 94, -13.5$) | -11.70 (dd, $J = 108, -14$) |
| DIPHOS-(3,5-CF ₃ ,2-CH ₃) (8) | 36.1 (br s) | 24.3 (dd, $J = 84, 11$) | 26.0 (br s) | 38.8 (d, $J = 93$) | -11.67 (dd, $J = 94, -14$) | -10.56 (dd, $J = 100, -14$) |
| DIPHOS-(2-CF ₃ ,2-CH ₃) (9) | 39.2 (br s) | 26.2 (d, $J = 98$) | 27.5 (br s) | 34. (d, $J = 101$) | -11.22 (dd, $J = 98, -15$) | -11.45 (dd, $J = 111, -17$) |
| | 2-CF ₃ | 2-CH ₃ | 2-CH ₃ | 2-CF ₃ | | |

^a For complete characterization see ref 16.

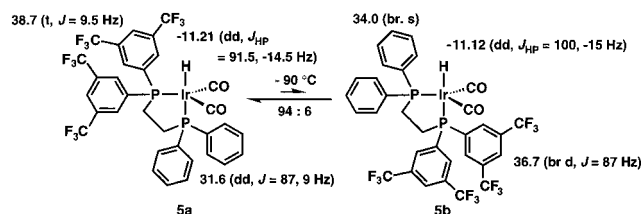


Figure 3. $[\text{DIPHOS}-(3,5\text{-CF}_3,\text{H})\text{Ir}(\text{CO})_2\text{H}$ (**5**) is an equilibrium mixture of two isomers.

shift of the apical phosphorus trans to hydride ($J_{\text{HP}} = 87$ Hz) is similar to the δ 37.4 ($J_{\text{HP}} = 103$ Hz) chemical shift of the apical phosphorus of $(\text{DIPHOS}-3,5\text{-CF}_3)\text{Ir}(\text{CO})_2\text{H}$ and the δ 34.0 (br s) chemical shift of its equatorial phosphorus cis to hydride is similar to the δ 33.6 (d, $J_{\text{HP}} = 12$ Hz) of the equatorial phosphine of $(\text{DIPHOS})\text{Ir}(\text{CO})_2\text{H}$. This establishes the structure of the minor isomer as **5b** with the electron-withdrawing PAr_2 group in an apical position.

The electron-withdrawing substituted diarylphosphine prefers the equatorial position as shown in the major isomer **5a**. A similar bias toward coordination of phosphines with electron-withdrawing groups in the equatorial position was responsible for an increase in the ratio of diequatorial to apical-equatorial isomers for T-BDCP-(3,5-CF₃) (**ae:ee** = 10:90) relative to T-BDCP (**ae:ee** = 63:37).¹⁶ Hoffmann's molecular orbital analysis of ligand electronic site preferences in five-coordinate d^8 ML_5 complexes²¹ also supports these observations, suggesting that weaker σ -donor ligands should prefer the equatorial position while stronger σ -donor ligands should prefer the apical position.

At room temperature, **5a** and **5b** undergo rapid interconversion and average resonances are observed in the NMR spectra. The hydride resonances average to give a doublet of doublets at δ -11.2 with average coupling constants of 75 and 5.5 Hz to the two different phosphines. The ^{31}P NMR spectrum shows averaged signals at δ 39.6 (d, $J_{\text{PP}} = 9$ Hz) and 32.5 (d, $J_{\text{PP}} = 9$ Hz) which were assigned to the averaged PAr_2 resonance and the averaged PPh_2 resonance, respectively.

The J_{PH} coupling constants of individual isomers **5a** and **5b** should be nearly temperature independent. In a rapidly equili-

brating mixture of **5a** and **5b**, the observed coupling constants are the weighted average of the coupling constants of the two isomers and can be used to compute the mole fraction of **5a** and **5b** present:

$$(J_{\text{PH}} \text{ at } 25^\circ\text{C}) = \chi_{5a}(J_{\text{PH}} \text{ in } \mathbf{5a} \text{ at } -94^\circ\text{C}) + \chi_{5b}(J_{\text{PH}} \text{ in } \mathbf{5b} \text{ at } -94^\circ\text{C}) \quad (1)$$

For the PPh_2 group, the +75 Hz room-temperature coupling constant for the equilibrating mixture of **5a** and **5b**, the 91.5 Hz for the low-temperature J_{PH} of **5a**, and the -14 Hz for the low-temperature J_{PH} of **5b** were inserted into eq 1 to give mole fractions $\chi_{5a} = 0.844$ and $\chi_{5b} = 0.156$.²² Similarly, the coupling constants for the PAr_2 group provided an independent measurement of $\chi_{5a} = 0.825$ and $\chi_{5b} = 0.175$ when the average room-temperature coupling constant of the PAr_2 group (+5.5 Hz) and the low-temperature coupling constants for **5a** (-14.5 Hz) and **5b** (100 Hz) were inserted into eq 1.²³ The average of these two independent measurements corresponds-to-a ratio of **5a**:**5b** of 83:17 at room temperature ($\Delta G^\circ = 0.94$ kcal mol⁻¹). At -94 °C, this ratio was 94:6 ($\Delta G^\circ = 0.97$ kcal mol⁻¹) (Table 2).

Additional (Diphosphine) $\text{Ir}(\text{CO})_2\text{H}$ Complexes. The remaining three complexes, $[\text{DIPHOS}-(2\text{-CF}_3,\text{H})\text{Ir}(\text{CO})_2\text{H}$ (**6**), $[\text{DIPHOS}-(3,5\text{-CF}_3,2\text{-CH}_3)\text{Ir}(\text{CO})_2\text{H}$ (**8**), and $[\text{DIPHOS}-(2\text{-CF}_3,2\text{-CH}_3)\text{Ir}(\text{CO})_2\text{H}$ (**9**), were characterized similarly to complex **5** above. Selectively hydride-coupled ^{31}P spectra were used to determine the site of phosphine binding, and ^{31}P chemical shifts of the isomers were assigned by comparison of shifts in dissymmetric complexes with the corresponding shifts for the symmetric complexes (Table 1). Ratios of isomers at low temperature were obtained by integration and ratios at room temperature by eq 1 (Table 2).²⁴⁻²⁶

(22) There are two possible solutions to each equation because the sign of J_{RT} is unknown. The solution of eq 1 gives $\chi_A = 0.844$ for +75 Hz or $\chi_A = -0.578$ for -75 Hz. The reasonable solution with $0 \leq \chi_A \leq 1$ is picked.

(23) In this case both solutions are reasonable, $\chi_A = 0.825$ or $\chi_A = 0.921$. The solution most similar to $\chi_A = 0.844$, obtained in the previous calculation, was selected.

(21) Rossi, A. R.; Hoffmann, R. *Inorg. Chem.* **1975**, *14*, 365.

Table 2. Isomer Ratios for Complexes 5–8 at Low Temperature and Room Temperature

| diphosphine | major hydride at low temp | minor hydride at low temp | low temp isomer ratio | hydride at room temp | room temp isomer ratio |
|--|--|-------------------------------------|-----------------------|------------------------------------|------------------------|
| DIPHOS–(3,5-CF ₃ ,H) (5) | –11.21 (dd, <i>J</i> = 91.5, –14.5) | –11.12 (dd, <i>J</i> = 100, –14) | 94:6 | –11.20 (dd, <i>J</i> = 75, 5.5) | 83:17 |
| DIPHOS–(2-CF ₃ ,H) (6) | –10.69 (dd, <i>J</i> = 94, –13.5) | –11.70 (dd, <i>J</i> = 108, –14) | 67:33 | –11.18 (dd, <i>J</i> = 57, 31) | 65:35 ²⁴ |
| DIPHOS–(3,5-CF ₃ ,2-CH ₃) (8) | –11.67 (dd, <i>J</i> = 94, –14) | –10.56 (dd, <i>J</i> = 100, –14) | 96:4 | –11.58 (dd, <i>J</i> = 82, 0) | 88:12 ²⁵ |
| DIPHOS–(2-CF ₃ ,2-CH ₃) (9) | –11.22 (dd, <i>J</i> = 98, –15) | –11.45 (dd, <i>J</i> = 111, –17) | 60:40 | –11.39 (dd, <i>J</i> = 62, 27) | 68:32 ²⁶ |

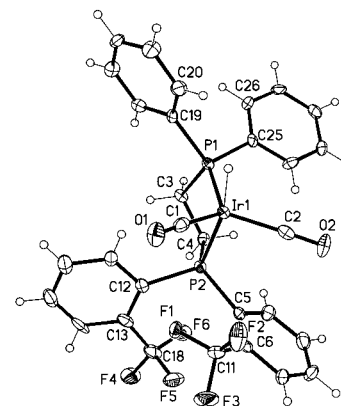
Table 3. Regiochemistry of Hydroformylation of 1-Hexene with Rhodium Diphosphine Catalysts

| diphosphine | Ir complex ratio ae-1:ae-2 ^a | aldehyde n:i ^b | regiochemistry % n | turnover rate ^c |
|--|--|---------------------------|--------------------|----------------------------|
| Symmetric Chelates | | | | |
| DIPHOS | 100:0 | 2.6:1 ± 0.1 | 71.9 ± 0.3 | 3.5 ± 0.1 |
| DIPHOS–(3,5-CF ₃) | 100:0 | 1.3:1 ± 0.1 | 56.9 ± 0.9 | 4.3 ± 0.1 |
| DIPHOS–(2-CH ₃) | 100:0 | 3.0:1 ± 0.1 | 75.2 ± 0.5 | 4.0 ± 0.2 |
| DIPHOS–(2-CF ₃) | 100:0 | 2.6:1 ± 0.1 | 72.1 ± 0.3 | 0.40 ± 0.01 |
| Dissymmetric Chelates | | | | |
| DIPHOS–(3,5-CF ₃ ,H) (1) | 83:17 | 4.2:1 ± 0.1 | 80.8 ± 0.3 | 2.5 ± 0.1 |
| DIPHOS–(2-CF ₃ ,H) (2) | 65:35 | 2.9:1 ± 0.1 | 74.1 ± 0.5 | 3.8 ± 0.2 |
| DIPHOS–(3,5-CF ₃ ,2-CH ₃) (3) | 88:12 | 3.3:1 ± 0.1 | 76.9 ± 0.6 | 4.7 ± 0.1 |
| DIPHOS–(2-CF ₃ ,2-CH ₃) (4) | 68:32 | 3.8:1 ± 0.1 | 79.1 ± 0.2 | 2.7 ± 0.1 |

^a Ratio of **ae-1:ae-2** isomers of (diphosphine)Ir(CO)₂H at room temperature. ^b Moles of heptanal:moles of 2-methylhexanal. ^c Turnover rate = [moles of aldehyde] × [moles of Rh]^{–1} h^{–1}.

In summary, all the (diphosphine)Ir(CO)₂H complexes are a mixture of two equilibrating isomers. For the key [DIPHOS–(3,5-CF₃,H)]Ir(CO)₂H complex (5) and for [DIPHOS–(3,5-CF₃,2-CH₃)]Ir(CO)₂H (8), which both have 3,5-CF₃-substituted arenes, the major isomers have the electron-withdrawing substituted phosphine in the equatorial position, with isomer ratios of 94:6 and 96:4, respectively. In the case of the *o*-trifluoromethyl-substituted arylphosphine complexes, [DIPHOS–(2-CF₃,H)]Ir(CO)₂H (6) and [DIPHOS–(2-CF₃,2-CH₃)]Ir(CO)₂H (9), with only one trifluoromethyl group per aryl, the preference for the isomers with the electron-withdrawing substituted phosphine in the equatorial position was less, with isomer ratios of 67:33 and 60:40, respectively. Steric effects are apparently insignificant, and the isomer preference is dictated by the number of electron-withdrawing trifluoromethyl substituents. In all cases, the major isomer has the electron-withdrawing substituted phosphine in the equatorial position and the better donor phosphine in the apical position. This is the preferred orientation to test our hypothesis.

X-ray Structure Determination of [DIPHOS–(2-CF₃,H)]-Ir(CO)₂H (6). Recrystallization of [DIPHOS–(2-CF₃,H)]Ir(CO)₂H (6) from pentane gave pale yellow plates, suitable for X-ray structure determination.²⁷ The X-ray crystal structure of 6 shows that the minor isomer 6b selectively crystallized from the 2:1 mixture of 6a:6b in solution. 6b has a trigonal bipyramidal structure, with the DIPHOS–(2-CF₃,H) ligand chelated in an apical–equatorial fashion, with bite angle 85.19(5)° [P(2)–Ir(1)–P(1)] (Figure 4). Similar Ir–P bond

**Figure 4.** ORTEP drawing of the X-ray crystal structure of [DIPHOS–(2-CF₃,H)]Ir(CO)₂H (6b).

lengths were observed for equatorial Ir–PPh₂ (2.310(2) Å) and for apical Ir–P[C₆H₃3,5-(CF₃)₂]₂ (2.331(2) Å). Although the hydride was not located directly, it is expected to occupy the other apical site. The angles between the apical phosphine and the equatorial carbonyls are 100.0° [C(1)–Ir(1)–P(2)] and 94.3° [C(2)–Ir(1)–P(2)], indicating the carbonyls are bent slightly toward the hydride ligand.

Catalytic Hydroformylation of 1-Hexene. As in our earlier studies, hydroformylation of 1-hexene was carried out in benzene solution at 36 °C under 6 atm of 1:1 H₂:CO using 0.2 mol % 1:1 Rh(CO)₂(acac):diphosphine catalyst. The production of heptanal and 2-methylhexanal was monitored by gas chromatography utilizing toluene as an internal standard. The results of the studies are summarized in Table 3. The turnover rate and n:i ratios are reported after 120–250 turnovers (20–50% conversion).

Discussion

The key dissymmetric diphosphine ligand DIPHOS–(3,5-CF₃,H) (1) shows an n:i ratio of 4.2:1, higher than either of the symmetric ligands DIPHOS, 2.6:1, and DIPHOS–(3,5-CF₃),

(24) Equation 1 for complex 6: ±57 Hz = χ_{6a} (94 Hz) + (χ_{6b})(–14 Hz), $\chi_A = 0.657$ or $\chi_A = -0.398$; and ±31 Hz = χ_{6a} (–13.5 Hz) + (χ_{6b})(108 Hz), $\chi_A = 0.634$ or $\chi_A = 1.144$.

(25) Equation 1 for 8: ±82 Hz = χ_A (94 Hz) + (1 – χ_A)(–14 Hz), $\chi_A = 0.889$ or $\chi_A = -0.630$; and 0 Hz = χ_A (–14 Hz) + (1 – χ_A)(100 Hz), $\chi_A = 0.877$.

(26) Equation 1 for 9: ±62 Hz = χ_A (98 Hz) + (1 – χ_A)(–17 Hz), $\chi_A = 0.687$ or $\chi_A = -0.391$; and ±27 Hz = χ_A (–15 Hz) + (1 – χ_A)(111 Hz), $\chi_A = 0.667$ or $\chi_A = 1.095$.

(27) The DIPHOS–(2-CF₃, H) ligand was further characterized by the synthesis and X-ray crystal structure determination of the [DIPHOS–(2-CF₃, H)]Fe(CO)₃ (7) complex. See the Supporting Information.

1.3:1. This observation of a significant synergistic effect with electronically dissymmetric ligands supports our hypothesis that electron-withdrawing groups in the equatorial position modestly increase *n:i* regioselectivity but electron-withdrawing groups in the apical position greatly decrease regioselectivity.

The increase in *n:i* selectivity for the dissymmetric diphosphine DIPHOS-(3,5-CF₃,H) (**1**) is attributed to the presence of an electron-withdrawing phosphine in an equatorial position which enhances *n:i* selectivity and the absence of an electron-withdrawing phosphine in the apical position which would have decreased *n:i* selectivity. The major isomer (83%) of the iridium model compound [DIPHOS-(3,5-CF₃,H)]Ir(CO)₂H (**5**) had the electron-withdrawing phosphine in the equatorial position. While it is unknown whether the two catalytic rhodium isomers react at similar rates, the small difference in rates for the symmetric diphosphines suggests that the two isomers of the dissymmetric chelate probably react at comparable rates.²⁸

The turnover rate for hydroformylation with **1** (2.5 turnovers h⁻¹) is slightly less than the rates with either of the symmetric diphosphines DIPHOS (3.5 turnovers h⁻¹) and DIPHOS-(3,5-CF₃) (4.3 turnovers h⁻¹). While the rate differences are small, we believe it is significant that the dissymmetric diphosphine has a rate outside the range of the related symmetric diphosphines.

The other three dissymmetric ligands **2–4** also achieve *n:i* ratios higher than the related symmetric complexes. DIPHOS-(2-CF₃,H) (**2**) gives an *n:i* ratio of 2.9:1, higher than either DIPHOS at 2.6:1 or DIPHOS-(2-CF₃) also at 2.6:1. Perhaps the smaller increase in selectivity is due to a more similar isomer ratio of 65:35. DIPHOS-(3,5-CF₃,2-CH₃) (**3**) gives an *n:i* ratio of 3.3:1, higher than either DIPHOS-(2-CH₃) at 3.0:1 or DIPHOS-(3,5-CF₃) at 1.3:1. And finally, DIPHOS-(2-CF₃,2-CH₃) (**4**) also gives an increased *n:i* ratio of 3.8:1 compared to its symmetric counterparts, DIPHOS-(2-CH₃) at 3.0:1 and DIPHOS-(2-CF₃) at 2.6:1.

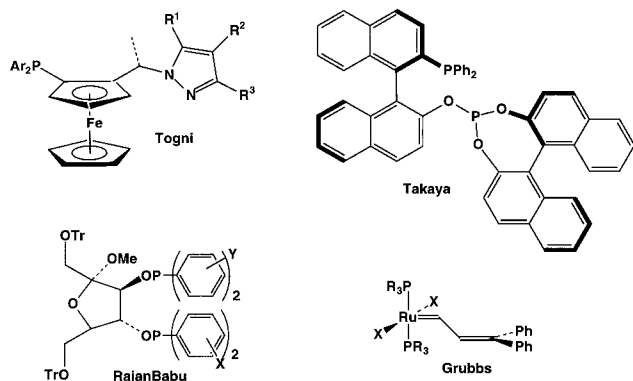


Figure 5. Electronically dissymmetric ligands and catalysts.

Enhanced product selectivity and more rapid rates for electronically dissymmetric ligands have been observed previously (Figure 5). Togni studied electronic effects on enantio-

(28) If it is assumed that the ratio of [DIPHOS-(3,5-CF₃, H)]Rh(CO)-(alkene)H isomers is the same as the 83:17 ratio of isomers of iridium complex **5**, and that both isomers react at the same rate, the *n:i* ratio derived from each of these rhodium isomers can be calculated. The 2.6:1 ratio seen for DIPHOS was assumed to be perturbed to 1.3:1 by both equatorial and apical phosphine substitution for DIPHOS-(3,5-CF₃). The ratio for DIPHOS was assumed to be perturbed by either an equatorial or an apical phosphine substitution for the two different isomers of DIPHOS-(3,5-CF₃,H) (**1**). The *n:i* ratio for the major isomer of [DIPHOS-(3,5-CF₃,H)]Rh(CO)(alkene)H which has the electron-withdrawing aryl groups on the equatorial phosphine was calculated to be 4.9 and the *n:i* ratio for the minor isomer with the electron-withdrawing aryl groups on the apical phosphine was calculated to be 0.7.

selectivity of rhodium-catalyzed hydroborations with pyrazole-containing ferrocenylphosphine ligands.²⁹ The combination of electron-withdrawing 3,5-(CF₃)₂ groups on the arylphosphine and electron donor groups on the pyrazole ring gave the highest enantioselectivity (98.5% ee for hydroboration of styrene). The opposite combination of CF₃ groups on the pyrazole ring and electron donor *p*-methoxy groups on the diarylphosphine gave the lowest enantioselectivity (5% ee). RajanBabu and Casalnuovo have used electronically unsymmetrical bis-3,4-diarylphosphinite ligands based on an α -D-fructofuranoside for asymmetric hydrocyanation.³⁰ The highest enantioselectivities for hydrocyanation to give naproxen nitrile (95% ee) were obtained with a dissymmetric bisdiarylphosphinite having a relatively electron-rich Ph₂P and an electron-poor [3,5-(CF₃)₂C₆H₃]₂P. Takaya reported that the electronically dissymmetric phosphine-phosphite ligand (BINAPHOS) gave unusually high enantioselectivity in hydroformylation.³¹ This ligand which has an electron-withdrawing phosphite ligand and an electron-donating phosphine gave 94% ee in the rhodium-catalyzed hydroformylation of styrene.

Grubbs found opposite electronic effects for halide and phosphine ligands on ruthenium metathesis catalysts. The fastest rates were observed for ruthenium olefin metathesis catalysts (PR₃)₂X₂Ru=CHR containing sterically large electron-donating phosphines (PCy₃ > P^tPr₃ > PCy₂Ph > PⁱPr₂Ph > PPh₃) and small electron withdrawing halide ligands (Cl > Br > I).³² It was suggested that the large electron-donating phosphines more readily dissociate to open a coordination site and that the electron-withdrawing halogens stabilize alkene binding.

Conclusions

DIPHOS-(3,5-CF₃,H) (**1**) shows a *n:i* ratio higher than either of the symmetric ligands DIPHOS or DIPHOS-(3,5-CF₃), supporting our hypothesis that creating an electronically dissymmetric environment about our hydroformylation catalysts enhances linear aldehyde selectivity. An electron-withdrawing substituent on an equatorial phosphine increases the *n:i* ratio while an electron-withdrawing substituent on an apical phosphine decreases the *n:i* ratio. Therefore, the best DIPHOS catalysts place an electron-withdrawing substituted phosphine in the equatorial position and an electron-donating substituted phosphine in the apical position.

Experimental Section

General Procedures. See the Supporting Information. Ir(acac)-(CO)₂,³³ Rh(CO)₂(acac),³⁴ (2-CH₃C₆H₄)₂PH,¹⁶ [3,5-(CF₃)₂C₆H₃]₂P(CH=CH₂),¹⁶ and (2-CF₃C₆H₄)₂P(CH=CH₂)¹⁶ were prepared as reported. Analyzed mixtures of 1:1 CO:H₂ were obtained from Matheson Gas Products or Liquid Carbonic.

[3,5-(CF₃)₂C₆H₃]₂PCH₂CH₂P(C₆H₅)₂, DIPHOS-(3,5-CF₃,H) (**1**). Following a procedure similar to that used for 1-(diphenylphosphino)-2-bis(*m*-fluorophenyl)phosphinoethane,³⁵ a mixture of (C₆H₅)₂PH (1.26 mL, 7.22 mmol), [3,5-(CF₃)₂C₆H₃]₂P(CH=CH₂) (3.50 g, 7.22 mmol),

(29) (a) Schnyder, A.; Hintermann, L.; Togni, A. *Angew. Chem., Int. Ed. Engl.* **1995**, *34*, 931. (b) Schnyder, A.; Togni, A.; Wiesli, U. *Organometallics* **1997**, *16*, 255.

(30) RajanBabu, T. V.; Casalnuovo, A. L. *J. Am. Chem. Soc.* **1996**, *118*, 6325.

(31) (a) Horiuchi, T.; Ohta, T.; Nozaki, K.; Takaya, H. *J. Chem. Soc., Chem. Commun.* **1996**, 155. (b) Sakai, N.; Mano, S.; Nozaki, K.; Takaya, H. *J. Am. Chem. Soc.* **1993**, *115*, 7033.

(32) Dias, E. L.; Nguyen, S. T.; Grubbs, R. H. *J. Am. Chem. Soc.* **1997**, *119*, 3887.

(33) Roberto, D.; Cariati, E.; Psaro, R.; Ugo, R. *Organometallics* **1994**, *12*, 4227.

(34) Varshavskii, Y. S.; Cherkasova, T. G. *Russ. J. Inorg. Chem.* **1967**, *12*, 899.

(35) Kapoor, P. N.; Pathak, D. D.; Gaur, G.; Kutty, M. *J. Organomet. Chem.* **1984**, *276*, 167.

and KO-*t*-Bu (0.3 g, 2.7 mmol) in THF (10 mL) was refluxed for 4 h. Solvent was evaporated, and the resulting brown residue was recrystallized twice from EtOH to give **1** (2.35 g, 49%) as a light cream solid: mp 75–78 °C; ^1H NMR (CD_2Cl_2 , 300 MHz) δ 7.90 (br s, para Ar), 7.79 (br d, $J = 6$ Hz, ortho Ar), 7.33–7.31 (m, Ph), 2.30–2.04 (m, CH_2CH_2); $^{13}\text{C}\{^1\text{H}\}$ NMR (CD_2Cl_2 , 125.7 MHz) δ 141.94 (d, $J_{\text{CP}} = 21.5$ Hz, ipso), 137.94 (d, $J_{\text{CP}} = 14$ Hz, ipso'), 133.11 (br d, $J_{\text{CP}} = 21.4$ Hz, ortho Ar), 132.92 (d, $J_{\text{CP}} = 18.6$ Hz, ortho Ph), 132.29 (qd, $J_{\text{CF}} = 33.2$ Hz, $J_{\text{CP}} = 5.9$ Hz, CCF_3), 129.9 (d, $J_{\text{CP}} = 6.8$ Hz, meta Ph), 129.38 (s, para Ph), 123.83 (br m, para Ar), 123.53 (q, $J_{\text{CF}} = 273$ Hz, CF_3), 24.24 (t, $J_{\text{CP}} = 16.6$ Hz, CH_2), 24.05 (t, $J_{\text{CP}} = 15.6$ Hz, CH_2'); $^{31}\text{P}\{^1\text{H}\}$ NMR (CD_2Cl_2 , 121 MHz) δ -9.58 (d, $J_{\text{PP}} = 39$ Hz, PAr_2), -13.00 (d, $J_{\text{PP}} = 39$ Hz, PPh_2); $^{19}\text{F}\{^1\text{H}\}$ NMR (CD_2Cl_2 , 282 MHz) δ -63.2 (s); HRMS (EI) calcd (obsd) for $\text{C}_{30}\text{H}_{20}\text{F}_{12}\text{P}_2$ 670.0849 (670.0846).

(2- $\text{CF}_3\text{C}_6\text{H}_4$) $_2\text{PCH}_2\text{CH}_2\text{P}(\text{C}_6\text{H}_5)_2$, DIPHOS-(2- CF_3 ,H) (2). A solution of (2- $\text{CF}_3\text{C}_6\text{H}_4$) $_2\text{P}(\text{CH}=\text{CH}_2)$ (9.0 g, 25.8 mmol), (C_6H_5) $_2\text{PH}$ (4.6 mL, 26.4 mmol), and KO-*t*-Bu (0.2 g, 1.8 mmol) in THF (20 mL) was refluxed for 2 h. Solvent was evaporated, and the resulting brown residue was recrystallized from EtOH to give **2** (3.3 g, 23%) as a pale yellow powder: mp 133–135 °C; ^1H NMR (CD_2Cl_2 , 300 MHz) δ 7.9–7.3 (m, Ar), 2.07 (m, CH_2CH_2); $^{13}\text{C}\{^1\text{H}\}$ NMR (CD_2Cl_2 , 125.7 MHz) δ 138.52 (d, $J_{\text{CP}} = 14.7$ Hz, ipso), 136.68 (d, $J_{\text{CP}} = 32.2$ Hz, ipso'), 134.3 (qd, $J_{\text{CF}} = 30.3$ Hz, $J_{\text{CP}} = 24.5$ Hz, CCF_3), 133.69 (s, Ar), 133.05 (d, $J_{\text{CP}} = 18.6$ Hz, ortho Ph), 132.10 (s, Ar), 129.38 (s, Ar), 129.14 (s, para Ph), 128.85 (d, $J_{\text{CP}} = 6.8$ Hz, meta Ph), 127.09 (s, Ar), 124.68 (q, $J_{\text{CF}} = 273$ Hz, CF_3), 24.86 (t, $J_{\text{CP}} = 17.6$ Hz, CH_2), 24.33 (dd, $J_{\text{CP}} = 18.6$, 14.7 Hz, CH_2'); $^{31}\text{P}\{^1\text{H}\}$ NMR (CD_2Cl_2 , 121 MHz) δ -12.3 (d, $J_{\text{PP}} = 33$ Hz, PPh_2), -22.8 (dsept, $J_{\text{PP}} = 33$ Hz, $J_{\text{PF}} = 50$ Hz, PAr_2); $^{19}\text{F}\{^1\text{H}\}$ NMR (CD_2Cl_2 , 282 MHz) δ -57.1 (d, $J_{\text{PF}} = 50$ Hz); EI mass spectrum m/z (%) 534 (74) [M^+], 550 (7) [MO^+], 405 (100).

[3,5-(CF_3) $_2\text{C}_6\text{H}_3$] $_2\text{PCH}_2\text{CH}_2\text{P}(\text{C}_6\text{H}_4\text{-2-CH}_3)_2$, DIPHOS-(3,5- CF_3 ,2- CH_3) (3). A solution of (2- $\text{CH}_3\text{C}_6\text{H}_4$) $_2\text{PH}$ (2.3 g, 10.8 mmol), [3,5-(CF_3) $_2\text{C}_6\text{H}_3$] $_2\text{P}(\text{CH}=\text{CH}_2)$ (5.3 g, 10.9 mmol), and KO-*t*-Bu (0.3 g, 2.7 mmol) in THF (20 mL) was refluxed for 4 h. Solvent was evaporated, and the resulting brown residue was recrystallized twice from benzene: MeOH to give **3** (4.6 g, 61%) as white fine crystalline needles: mp 131–132 °C; ^1H NMR (CD_2Cl_2 , 300 MHz) δ 7.89 (s, para, Ar), 7.79 (d, $J_{\text{PH}} = 6.3$ Hz, ortho, Ar), 7.10 (m, 4H, tol), 2.36 (s, CH_3), 2.29 (m, CH_2CH_2), 2.20 (m, $\text{CH}_2\text{CH}_2'$); $^{13}\text{C}\{^1\text{H}\}$ NMR (CD_2Cl_2 , 125.7 MHz) δ 142.9 (d, $J_{\text{CP}} = 26$ Hz, ipso), 141.1 (d, $J_{\text{CP}} = 22.4$ Hz, ipso'), 136.1 (d, $J_{\text{CP}} = 13.5$ Hz, ortho Ar), 133.1 (d, $J_{\text{CP}} = 18$ Hz, ortho tol), 132.4 (qd, $J_{\text{CF}} = 33$ Hz, $J_{\text{CP}} = 5.4$ Hz, CCF_3), 131.2 (s), 130.7 (d, $J_{\text{CP}} = 3.6$ Hz), 129.2 (s), 126.6 (s), 123.9 (s, para tol), 123.6 (q, $J_{\text{CF}} = 273$ Hz, CF_3), 24.5 (t, $J_{\text{CP}} = 16$ Hz, CH_2), 22.8 (t, $J_{\text{CP}} = 15$ Hz, CH_2'), 21.3 (d, $J_{\text{CP}} = 22$ Hz, CH_3); $^{31}\text{P}\{^1\text{H}\}$ NMR (CD_2Cl_2 , 202 MHz) δ -9.7 (d, $J_{\text{PP}} = 40$ Hz, PAr_2), -33.9 [d, $J_{\text{PP}} = 40$ Hz, $\text{P}(o\text{-Tol})_2$]; $^{19}\text{F}\{^1\text{H}\}$ NMR (282 MHz, CD_2Cl_2) δ -63.2 (s); EI mass spectrum m/z (%) 698 (100) [M^+], 679 (14) [$\text{M} - \text{F}^+$]. Anal. Calcd for $\text{C}_{32}\text{H}_{24}\text{F}_{12}\text{P}_2$: C, 55.03; H, 3.46. Found: C, 54.80; H, 3.53.

(2- $\text{CF}_3\text{C}_6\text{H}_4$) $_2\text{PCH}_2\text{CH}_2\text{P}(\text{C}_6\text{H}_4\text{-2-CH}_3)_2$, DIPHOS-(2- CF_3 ,2- CH_3) (4). A solution of (2- $\text{CH}_3\text{C}_6\text{H}_4$) $_2\text{PH}$ (1.20 g, 5.6 mmol), (2- $\text{CF}_3\text{C}_6\text{H}_4$) $_2\text{P}(\text{CH}=\text{CH}_2)$ (1.95 g, 5.6 mmol), and KO-*t*-Bu (0.2 g, 1.8 mmol) in THF (15 mL) was refluxed for 20 h. Solvent was evaporated, and the resulting brown residue was recrystallized twice from EtOH and then from EtOH: CH_2Cl_2 to give **4** (0.51 g, 16%) as a light cream solid: mp 178–181 °C; ^1H NMR (CD_2Cl_2 , 300 MHz) δ 7.8–7.7 (m, 2H), 7.53–7.43 (m, 4H), 7.28–7.00 (m, 10H), 2.38 (s, CH_3), 2.07 (t, $J = 4.2$ Hz, CH_2CH_2); $^{13}\text{C}\{^1\text{H}\}$ NMR (CD_2Cl_2 , 125.7 MHz) δ 142.78 (d, $J_{\text{CP}} = 25.4$ Hz, ipso); 136.80 (d, $J_{\text{CP}} = 16.6$ Hz, ipso'); 133.64, 132.10, 131.40, 130.42, 130.11, 129.34, 129.00, 128.93, 127.09, 126.42, 125.91, (Ar); 124.67 (q, $J_{\text{CF}} = 275$ Hz, CF_3); 24.83 (t, $J_{\text{CP}} = 16$ Hz, CH_2); 23.46 (t, $J_{\text{CP}} = 16$ Hz, CH_2'); 21.33 (d, $J_{\text{CP}} = 21$, CH_3); $^{31}\text{P}\{^1\text{H}\}$ NMR (CD_2Cl_2 , 121 MHz) δ -21.1 (dsept, $J_{\text{PP}} = 33$ Hz, $J_{\text{PF}} = 49$ Hz $\text{P}[2\text{-(CF}_3\text{)C}_6\text{H}_4]_2$), -32.0 (d, $J_{\text{PP}} = 33$ Hz, $\text{P}[(\text{CH}_3\text{)C}_6\text{H}_4]_2$); $^{19}\text{F}\{^1\text{H}\}$ NMR (CD_2Cl_2 , 282.16 MHz) δ -57.1 (d, $J_{\text{PF}} = 50$ Hz); HRMS (EI) calcd (obsd) for $\text{C}_{30}\text{H}_{26}\text{F}_6\text{P}_2$ 562.1414 (562.1416).

[DIPHOS-(3,5- CF_3 ,H)] $\text{Ir}(\text{CO})_2\text{H}$ (5). $\text{Ir}(\text{CO})_2(\text{acac})$ (2.9 mg, 8.4 μmol) and DIPHOS-(3,5- CF_3 ,H) (**1**) (5.7 mg, 8.5 μmol) in CD_2Cl_2 were shaken in an NMR tube for 20 h under 1 atm of 1:1 $\text{CO}:\text{H}_2$ to give a solution of **5**: ^1H NMR (CD_2Cl_2 , 500 MHz) δ 8.2–6.9 (m, Ar),

2.65–2.45 (CH_2CH_2), -11.20 (dd, $J_{\text{HP}} = 75$, 5.5 Hz, IrH); $^{13}\text{C}\{^1\text{H}\}$ NMR (CD_2Cl_2 , 125.7 MHz) δ 181.77 (dd, $J_{\text{CP}} = 30$, 6 Hz, CO), 139.75 (d, $J_{\text{CP}} = 37$ Hz, ipso), 134.34 (d, $J_{\text{CP}} = 46$ Hz, ipso'), 132.94 (br m), 132.7 (s), 132.57 (br d, $J_{\text{CP}} = 13.7$ Hz, ortho), 132.31 (d, $J_{\text{CP}} = 11.8$ Hz, ortho'), 131.19 (s, para Ph), 129.38 (br m), 129.09 (d, $J_{\text{CP}} = 10.6$ Hz, meta Ph), 126.1 (s), 124.96 (br s, para Ar), 123.36 (q, $J_{\text{CF}} = 273$ Hz, CF_3), 32.46 (dd, $J_{\text{CP}} = 34.2$, 21.5 Hz, CH_2), 31.51 (dd, $J_{\text{CP}} = 31.2$, 16.6 Hz, CH_2'); $^{31}\text{P}\{^1\text{H}\}$ NMR (CD_2Cl_2 , 202 MHz) δ 39.6 (d, $J_{\text{PP}} = 9$ Hz); 32.5 (d, $J_{\text{PP}} = 9$ Hz); $^{19}\text{F}\{^1\text{H}\}$ NMR (282 MHz, CD_2Cl_2) δ -63.2 (s); IR (CH_2Cl_2) 1992 (ν_{CO}), 1941 (ν_{CO}), 2067 ($\nu_{\text{Ir-H}}$) cm^{-1} .

^1H NMR (CD_2Cl_2 , 500 MHz, -94 °C) δ 8.2–6.9 (m, Ar), 2.67–2.37 (m, CH_2CH_2), -11.21 (dd, $J_{\text{HP}} = 91.5$, -14.5 Hz, IrH, **5a**), -11.12 (dd, $J_{\text{HP}} = 100$, -14 Hz, IrH, **5b**); the ratio of **5a**:**5b** IrH resonances was 94:6; $^{31}\text{P}\{^1\text{H}\}$ NMR (CD_2Cl_2 , 202 MHz, -90 °C) (**5a**) δ 38.7 (d, $J_{\text{PP}} = 6$ Hz), 31.6 (d, $J_{\text{PP}} = 6$ Hz); (**5b**) δ 36.6 (br s), 34.1 (br s); the ratio of **5a**:**5b** was 94:6; $^{31}\text{P}\{^1\text{H}\}$ decoupled, except for the hydride region} NMR (CD_2Cl_2 , 202 MHz, -90 °C) (**5a**) δ 38.7 (t, $J_{\text{PH}} = 9.5$ Hz, $J_{\text{PP}} = 9.5$ Hz), 31.6 (dd, $J_{\text{PH}} = 87$ Hz, $J_{\text{PP}} = 9$ Hz); (**5b**) δ 36.7 (br d, $J_{\text{PH}} = 87$ Hz), 34.0 (br s).

[DIPHOS-(2- CF_3 ,H)] $\text{Ir}(\text{CO})_2\text{H}$ (6). Following a procedure similar to that used for (DIPHOS) $\text{Ir}(\text{CO})_2\text{H}$,¹⁹ a solution of NaBH_4 (170 mg, 4.54 mmol) in ethanol (20 mL) was added to a solution of [DIPHOS-(2- CF_3 ,H)] $\text{Ir}(\text{CO})_2\text{H}$ ³⁶ (400 mg, 0.454 mmol) in CH_2Cl_2 (10 mL). After 1 h, silica gel (1 g) and H_2O (100 μL) were added. The light yellow solution was filtered and evaporated to give [DIPHOS-(2- CF_3 ,H)] $\text{Ir}(\text{CO})_2\text{H}$ ³⁷ as a white solid. A suspension of the white solid in benzene in a quartz photolysis cell was purged with CO, and photolyzed for 3 h at 36 °C in a Rayonet photoreactor. Solvent was evaporated to give **6** as a yellow-orange oily solid that was then recrystallized from pentane to give single crystals suitable for X-ray diffraction.³⁸ ^1H NMR (500 MHz, CD_2Cl_2) δ 8.15–7.40 (m, Ar), 2.75–2.40 (m, CH_2CH_2), -11.18 (dd, $J_{\text{HP}} = 57$, 31 Hz, IrH); $^{31}\text{P}\{^1\text{H}\}$ NMR (202 MHz, CD_2Cl_2) δ 43.1 (br), 32.2 (br); $^{19}\text{F}\{^1\text{H}\}$ NMR (282 MHz, CD_2Cl_2) δ -55.3 (s); IR (CH_2Cl_2) 2049 (ν_{IrH}), 1980 (ν_{CO}), 1929 (ν_{CO}) cm^{-1} . Anal. Calcd for $\text{C}_{30}\text{H}_{24}\text{F}_6\text{IrO}_2\text{P}_2$: C, 45.98; H, 2.96. Found: C, 45.67; H, 3.07.

^1H NMR (500 MHz, CD_2Cl_2 , -106 °C) δ 8.87–7.15 (m, Ar), 3.6–2.5 (CH_2CH_2), -10.69 (dd, $J_{\text{HP}} = 94$, -13.5 Hz, IrH, **6a**), -11.70 (dd, $J_{\text{HP}} = 108$, -14 Hz, IrH, **6b**); the ratio of **6a**:**6b** IrH resonances was 67:33; $^{31}\text{P}\{^1\text{H}\}$ NMR (202 MHz, CD_2Cl_2 , -98 °C) (**6a**) δ 40.5 (s), 34.0 (s); (**6b**) δ 33.4 (s), 31.2 (s); the ratio of **6a**:**6b** was 67:33; $^{31}\text{P}\{^1\text{H}\}$ decoupled, except for the hydride region} NMR (CD_2Cl_2 , 202 MHz, -98 °C) (**6a**) δ 40.5 (s), 34.0 (d, $J_{\text{PH}} = 92$ Hz); (**6b**) δ 33.4 (d, $J_{\text{PH}} = 104$ Hz), 31.2 (s).

[DIPHOS-(3,5- CF_3 ,2- CH_3)] $\text{Ir}(\text{CO})_2\text{H}$ (8). A benzene solution of [[DIPHOS-(3,5- CF_3 ,2- CH_3)] $\text{Ir}(\text{CO})_2\text{H}$]³⁶ (150 mg, 0.163 mmol) in a quartz photolysis cell purged with CO was photolyzed for 30 min at 36 °C. Solvent was evaporated to give **8** (60 mg, 39%) as a pale yellow solid: ^1H NMR (CD_2Cl_2 , 300 MHz) δ 8.20–7.15 (m, Ar), 2.70–2.37 (m, CH_2CH_2), 2.06 (s, CH_3), -11.58 (d, $J_{\text{HP}} = 82$ Hz, IrH); $^{31}\text{P}\{^1\text{H}\}$ NMR (CD_2Cl_2 , 121 MHz) δ 37.7 (d, $J_{\text{PP}} = 11$ Hz), 26.2 (d, $J_{\text{PP}} = 11$ Hz); $^{13}\text{C}\{^1\text{H}\}$ NMR (CD_2Cl_2 , 75 MHz) δ 182.1 (d, $J_{\text{CP}} = 32$ Hz, CO), 140.6 (d, $J_{\text{CP}} = 6$ Hz, ipso), 140.0 (dd, $J_{\text{CP}} = 37$, 2 Hz, ipso'), 140–123 (Ar), 123.4 (q, $J_{\text{CF}} = 271$ Hz, CF_3), 24.4 (d, $J_{\text{CP}} = 26$ Hz, CH_2), 23.3 (d, $J_{\text{CP}} = 22$ Hz, CH_2'), 22.1 (d, $J_{\text{CP}} = 7$ Hz, CH_3); $^{19}\text{F}\{^1\text{H}\}$ NMR (CD_2Cl_2 , 282 MHz) δ -63.2 (s); IR (CH_2Cl_2) 2028 (ν_{IrH}), 1988 (ν_{CO}), 1938 (ν_{CO}) cm^{-1} ; EI mass spectrum m/z (%) 919 (0.6) [$\text{M} - \text{CO}, \text{H}^+$], 918 (1.8) [$\text{M} - 2\text{Me}^+$], 888 (1.5) [$\text{M} - \text{CO}, \text{H}, 2\text{Me}^+$], 214 (100) [$\text{P}(\text{C}_6\text{H}_4\text{-2-CH}_3)_2$].

^1H NMR (500 MHz, CD_2Cl_2 , -110 °C) δ 8.7–6.9 (m, Ar); 3.2–2.8 (m, CH_2CH_2); 2.06 (s, CH_3 , major isomer), 1.75 (s, CH_3' , major isomer), -10.56 (dd, $J_{\text{HP}} = 100$, -14 Hz, IrH, **8b**), -11.67 (dd, $J_{\text{HP}} = 94$, -14 Hz, IrH, **8a**); the ratio of **8a**:**8b** was 96:4; $^{31}\text{P}\{^1\text{H}\}$ NMR (CD_2Cl_2 , 202 MHz, -106 °C) (**8a**) δ 36.1 (d, $J_{\text{PP}} = 11$ Hz), 24.3 (d, $J_{\text{PP}} = 11$ Hz); (**8b**) δ 38.8 (br s), 26.0 (br s); the ratio of **8a**:**8b** was 96:4. $^{31}\text{P}\{^1\text{H}\}$ decoupled, except for the hydride region} NMR (CD_2Cl_2 , 202 MHz, -110 °C) (**8a**) δ 36.1 (br s), 24.3 (dd, $J_{\text{PH}} = 84$ Hz, $J_{\text{PP}} = 11$ Hz); (**8b**) 38.8 (br d, $J_{\text{PH}} = 93$ Hz), 26.0 (br s).

(36) See the Supporting Information for synthesis and characterization.

(37) See the Supporting Information for characterization.

(38) See the Supporting Information for X-ray data.

[DIPHOS-(2-CF₃,2-CH₃)]Ir(CO)₂H (9**).** A benzene solution of [DIPHOS-(2-CF₃,2-CH₃)]Ir(CO)H₃³⁶ (50 mg, 0.064 mmol) was photolyzed in a quartz photolysis cell purged with CO for 30 min at 36 °C. Solvent was evaporated to give **9** (20 mg, 38%) as a brown oil: ¹H NMR (CD₂Cl₂, 500 MHz) δ 8.16–7.00 (m, Ar), 2.74–2.52 (m, CH₂CH₂), 2.01 (s, CH₃), –11.39 (dd, *J*_{HP} = 62, 27 Hz, IrH); ³¹P{¹H} NMR (CD₂Cl₂, 121 MHz) δ 42.6 (br s), 27.9 (br s); ¹³C{¹H} NMR (CD₂Cl₂, 125.7 MHz) δ 184.1 (br s, CO), 140.7 (d, *J*_{CP} = 5.9 Hz, ipso), 135.3 (d, *J*_{CP} = 6.5 Hz, ipso'), 132.3 (d, *J*_{CP} = 6.3 Hz), 131.6 (d, *J*_{CP} = 13 Hz), 130.9 (s), 130.7 (s), 129.0 (s) 128.7 (m), 126.28 (d, *J*_{CP} = 12.7 Hz), 124.5 (q, *J*_{CF} = 275 Hz, CF₃), 33.6 (m, CH₂), 33.3 (dd, *J*_{CP} = 33, 20 Hz, CH₂'), 22.0 (d, *J*_{CP} = 7 Hz, CH₃); ¹⁹F{¹H} NMR (282 MHz, CD₂Cl₂) δ –55.5 (s); IR (CH₂Cl₂) 2049 (*ν*_{Ir–H}), 1978 (*ν*_{CO}), 1926 (*ν*_{CO}) cm^{–1}.

¹H NMR (500 MHz, CD₂Cl₂, –98 °C) δ 8.8–6.9 (m, Ar); 3.3–2.6 (m, CH₂CH₂); 1.99 (s, CH₃, **9a**), 1.85 (s, CH₃, **9b**), 1.80 (s, CH₃', **9b**), 1.75 (s, CH₃', **9a**), –11.22 (dd, *J*_{HP} = 98, –15 Hz, **9a**), –11.45 (dd, *J*_{HP} = 111, –17 Hz, **9b**); the ratio of **9a**:**9b** was 60:40. The observation of more than one CH₃ resonance for each isomer may be due to hindered rotation about P–Ar bonds which gives rise to multiple rotomers, some with inequivalent CH₃ groups. ³¹P{¹H decoupled, except for the hydride region} NMR (CD₂Cl₂, 202 MHz, –98 °C) (**9a**) δ 39.2 (br s), 26.2 (d, *J*_{PH} = 98 Hz); (**9b**) δ 34.9 (br d, *J*_{PH} = 101 Hz), 27.5 (br s).

Catalytic Hydroformylation of 1-Hexene. Hydroformylation reactions were performed as described earlier in a 90-mL Fischer–Porter bottle equipped with a star-head magnetic stir bar.¹² Rh(CO)₂(acac) (10 mg, 39 μmol) and a chelating diphosphine (39 μmol) were dissolved in benzene (6.0 mL) under 70 psig of 1:1 CO:H₂ (50.02% CO, 49.98%

H₂) with toluene (0.20 mL, 1.9 mmol) added as an internal GC standard. After 1 h of stirring at 36 ± 2 °C, 1-hexene (2.50 mL, 0.020 mmol) was added. Samples containing heptanal and 2-methylhexanal were analyzed by temperature-programmed gas chromatography on an HP5890A chromatograph interfaced to a HP3390A integrator using an HP-1 10 m × 0.53 mm methyl silicone capillary column.

Acknowledgment. Financial support from the Department of Energy, Office of Basic Energy Sciences, is gratefully acknowledged. E.W.B. thanks the Fulbright commission for a fellowship. B.R.P. thanks the Alexander von Humboldt Stiftung for a von Lynene Fellowship. Grants from NSF (CHE-9105497) and from the University of Wisconsin for the purchase of the X-ray instruments and computers are acknowledged. We thank Alpha Aesar for a loan of iridium compounds.

Supporting Information Available: General experimental methods and experimental details and characterization for **7**, [DIPHOS-(2-CF₃,H)]Ir(CO)H₃, [DIPHOS-(2-CF₃,H)]Ir(CO)I, [DIPHOS-(3,5-CF₃,2-CH₃)]Ir(CO)I, [DIPHOS-(2-CF₃,2-CH₃)]-Ir(CO)I, [DIPHOS-(3,5-CF₃,2-CH₃)]Ir(CO)H₃, and [DIPHOS-(2-CF₃,2-CH₃)]Ir(CO)H₃ and X-ray crystallographic data for **6** and **7** (26 pages, print/PDF). See any current masthead page for ordering information and Web access instructions.

JA982117H